ELSEVIER

Applied Surface Science 184 (2001) 161–166

applied surface science

www.elsevier.com/locate/apsusc

Composition analysis of SiO_2/SiC interfaces by electron spectroscopic measurements using slope-shaped oxide films

Y. Hijikata[a,*], H. Yaguchi[a], M. Yoshikawa[b], S. Yoshida[a]

[a]*Faculty of Engineering, Department of Electrical and Electronic Systems Engineering, Saitama University, 255 Shimo-Okubo, Saitama-shi, Saitama 338-8570, Japan*

[b]*Japan Atomic Energy Research Institute, Takasaki Radiation Chemistry Research Establishment, 1233 Watanuki-machi, Takasaki-shi, Gunma 370-1292, Japan*

Abstract

We have characterized SiO_2/SiC interfaces by X-ray photoelectron spectroscopy in terms of composition and bonds to clarify the reasons for the problems in silicon carbide metal-oxide-semiconductor field-effect-transistor and MOS structures. The oxide films on 6H–SiC were shaped into slopes by HF chemical etching to obtain the depth profile of the composition and the bondings. An interface layer was found near the SiO_2/SiC boundary, where SiO_2 stoichiometry is collapsed and there exists the bondings other than Si–O_2 and Si–C. Also, we revealed the differences in the interface properties for different oxidation processes. © 2001 Elsevier Science B.V. All rights reserved.

Keywords: 6H–SiC; Oxidation; Slope-shaped oxide film; SiO_2/SiC interface; XPS; Bonding

1. Introduction

Silicon carbide metal-oxide-semiconductor field-effect-transistors (SiC MOSFETs) have some problems to be solved before practical use, such as their low channel mobilities and higher on-resistances than those predicted, nevertheless bulk SiC possesses superior characteristics. It has been reported [1] that the high interface trap density and high oxide-trapped charges of SiC MOS structures are concerned with the inferior properties of SiC MOSFETs. To overcome these problems, many ideas have been proposed for the fabrication process of SiC MOS structures, such as re-oxidation [2], post-oxidation annealing in hydrogen atmosphere [3], and utilization of low temperature oxide film deposition [4]. Many studies on the characterization of SiC/oxide layer interfaces have also been carried out by *C–V* measurements [5,6], internal photoemission spectroscopy (IPS) [7], spectroscopic ellipsometry [8], X-ray photoelectron spectroscopy (XPS) [9–13]. Afanas'ev and coworkers [14] suggested the existence of carbon clusters at the oxide/SiC interface from the observation of atomic force microscope (AFM) after removing the oxide layers. Several reports have pointed out [10–12] that there exists silicon oxycarbide (SiC_xO_y) with the thickness of 0.3–1 nm at the interface. While, recent report revealed that there is no excess carbon in the oxide or at the interface. However, the oxide is structurally different from that grown on Si though the oxide is stoichiometric SiO_2 [13]. In addition, Si–Si bonds remain at the interface after CO loses through the

* Corresponding author. Present address: Faculty of Engineering, Department of Electrical and Electronic Systems Engineering, Saitama University, 255 Shimo-Okubo, Saitama-shi, Saitama 338-8570, Japan. Tel./fax: +81-48-858-3822.
E-mail address: yasuto@opt.ees.saitama-u.ac.jp (Y. Hijikata).

0169-4332/01/$ – see front matter © 2001 Elsevier Science B.V. All rights reserved.
PII: S0169-4332(01)00491-3

oxidation [15]. For the discussion mentioned above, we are forced to say that obvious proof for inferior MOS properties of SiC has not been obtained yet.

In this report, we performed XPS measurements to study SiC/oxide interfaces using slope-shaped oxide films. Utilizing the slope-shaped oxide films, oxide film of various thicknesses with the same thermal history can be obtained by changing the measuring point. Moreover, this method is suitable for acquiring the information about the interface rather than depth profiling by ion sputtering, since the surface roughness is rather less than that by ion sputtering. Additionally, carbon atoms in SiC is often etched selectively by sputtering atom, e.g. positive argon ions, since carbon atoms are usually lighter than sputtering atoms. The interface between dry thermal oxide layer and 6H–SiC were characterized by monitoring the photoelectron spectra at the thin oxide region. Consequently, the structure of oxide near the interface is found to be different from stoichiometric SiO_2. In addition, other photoemission peaks in O-1s and C-1s core levels as well as O_2–Si or C–Si were detected. We have also discussed the bonding configuration of the interface from these experimental results.

2. Experimental details

6H–SiC epilayers, 5 μm in thickness and 5×10^{15} cm^{-3} in carrier density (n-type) (Cree), were cleaned by a standard RCA cleaning process and a native oxide on the surface was removed by buffered HF. Si(0 0 0 1) surfaces were oxidized in the flow of oxygen gas, the flow rate of which was 1000 sccm. The samples were cooled down immediately after the oxidation ceased. A spectroscopic ellipsometer was employed as a thickness monitor of oxide. The thickness was 36 nm in the case of oxidation for 6.5 h at 1100 °C. The oxide films were shaped into slope by dropping them gradually into a buffered HF bath [16]. The construction of the sloped oxide film used in this experiment is shown in Fig. 1. As shown in this figure, the gradient of fabricated slope-shaped oxide film was around 3 nm/mm, and whole length of the slope was 12 mm. To avoid the native oxidation of the etched surface in the atmosphere, 1 nm thick oxide layer was remained even at the most etched part. The mophorogies of the etched surfaces were examined by AFM

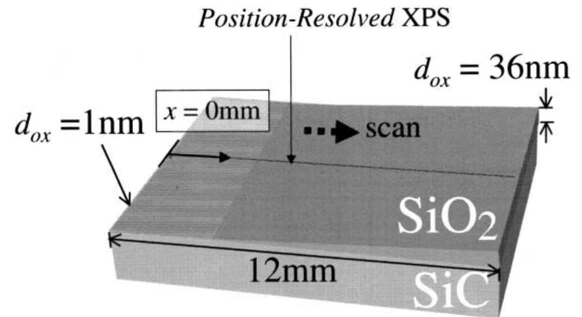

Fig. 1. The construction of the sloped shaped oxide film on 6H–SiC.

measurements. The root mean square (rms) values of the surface roughness were less than 0.3 nm.

XPS measurements were performed using Mg X-rays ($h\nu = 1253.6\,eV$). Photoelectrons from Si-2p, C-1s, and O-1s core levels were collected using a hemispherical analyzer with 50 eV pass energy, a 200 ms integration time, and 0.1 eV steps. An acceptance aperture was used to permit only photoelectrons emitted from $1 \times 1\,mm^2$.

3. Experimental results and discussions

Fig. 2(a) shows Si-2p photoelectron spectra as a function of the *x*-position illustrated in Fig. 1. The horizontal axis representing binding energy (E_b) was aligned by referring to E_b of C–Si bonding (=283.1 eV) which does not depend on the oxide thickness. The peaks corresponding to Si–C bonds (Si^+) were clearly seen at thin oxide region with $E_b = 100.6\,eV$, as well as Si–O_2 bond (Si^{4+}) with $E_b = 103.4\,eV$. Fig. 2(b) shows C-1s spectra as a function of the *x*-position. Two peaks for C–Si and $(CH_3)_n$ were clearly seen at $E_b = 283.1$ and 284.8 eV, respectively. Fig. 2(c) shows O-1s spectra as a function of the *x*-position. The peaks corresponding to O_2–Si bond ($E_b = 534.0\,eV$) were clearly seen, however, another peaks (O′) in the lower energy ($E_b \sim 531.0\,eV$) were detected when the *x*-position was less than 2.0 mm. We could not detect O′ peak on the surface of SiC nor that of thick oxide on SiC. Thus, photoelectrons arising O′ peaks must come from, not adsorptions of O atoms on the surface, but the interface layer. O′ peaks are explained by several structural

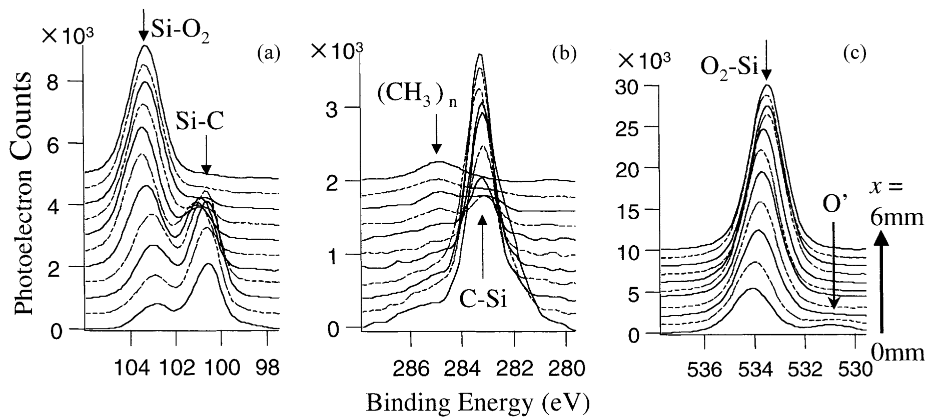

Fig. 2. Photoelectron spectra as a function of x-position: (a) Si-2p; (b) C-1s; (c) O-1s.

models at present. C–O–C or Si–O–Si bridges, or an insertion of O atom into the back-bond of Si (Si–O–C) have a possibility to bring about O′ peaks. In the case of Si, it has already been reported in SiO_2/Si interface [17] that a Si–O–Si bridge was found at lower E_b side than that of O_2–Si. Taking account that the substrate was Si face of 6H–SiC, C–O–C bridges is unlikely to exist. However, E_b shift of ~3 eV is too high to attribute Si–O–Si nor Si–O–C bridges. Paying an attention to E_b of O′, single oxygen atom is the most probable explanation. However, it is difficult to decide the origin of O′ peak clearly at present.

Next, the photoelectron spectra were deconvoluted to obtain the atomic concentrations and the binding energies of these peaks precisely. Examples of the fitting results ($x = 0.5$ mm) are shown in Fig. 3(a)–(c). An ordinary Gaussian function was used for the deconvolution process. It is very interesting that, by this analysis, the peaks corresponding to Si–Si bond (Si^{0+}, $E_b = 98.9$ eV) and Si–O–C bond (Si^{x+}, $E_b = 101.5$ eV) were found in Si-2p spectra, when the x-position was less than 1.5 mm, though its peak intensity was very weak. Moreover, a C-1s peak in a higher energy side ($E_b = 285.7$ eV) corresponding to C–O bond and another peak (C′) in a lower energy side ($E_b \sim 281.5$ eV) were detected when the x-position was less than 2.0 mm. C′ peaks cannot be explained by the existence of Si–O–C bonds, i.e. oxycarbide, because the C′ peak exists in lower E_b than C–Si peak. Oxygen atoms pull electron density away from C due to their high electro-negativity, resulting in

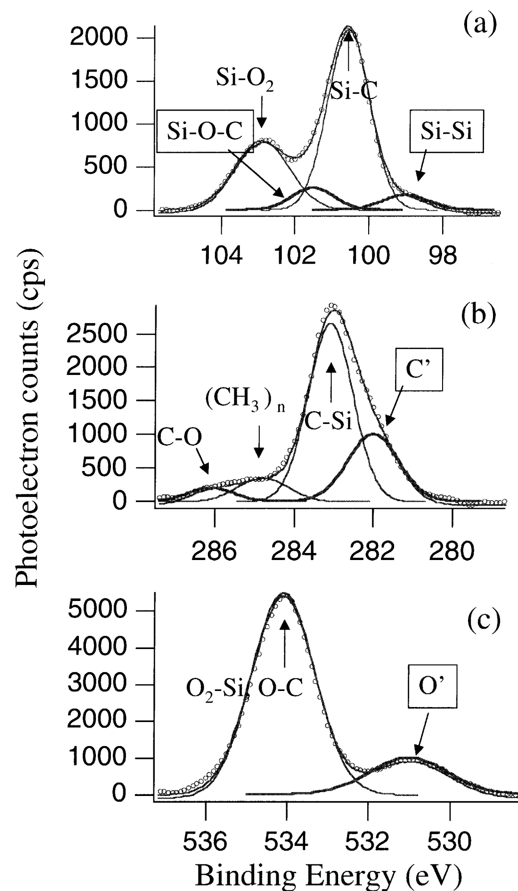

Fig. 3. The results of deconvolution process for: (a) Si-2p; (b) C-1s; (c) O-1s.

requiring more energy to photoeject core level electrons from C. Thus, if the C′ peak is caused by the existence of Si–O–C bonds, it must appear at higher E_b than C–Si peak. If the C′ peak is caused by Si–Si bonds at the interface region, E_b of C′ should change since the photoelectrons which come from carbon atoms in Si–Si*–C* (* denotes an atom in the second bilayer) are affected by different atomic arrangements from those in bulk SiC. While, C–O bonds may induce interfacial strain and/or electrostatic interaction. The former originates from the result of the evolution of gaseous CO through the oxide, and the latter is due to strong dipole moment of C–O bonds [13]. It can be also considered that C′ is not another peak but only the broadening of C–Si peak. Table 1 summarizes E_b and FWHM values of the photoelectron peaks.

The oxide thickness can be calculated by the photoelectron count ratio of Si^{4+} to Si^{+} and using the equations mentioned in Refs. [10,12]. Fig. 4 shows the oxide thickness measured by XPS as well as those by spectroscopic ellipsometry with respect to the x-position. They agreed with each other when $x < 3.5$ mm (oxide thickness < 6 nm). However, they do not agree where the oxide thickness is more than 6 nm. The reason for this discrepancy can be considered that the thickness measured by XPS contains large errors for thick oxide film, since the photoelectron signal of Si^{+} is very weak when the oxide thickness is over the escape depth of photoelectrons. At the x-position of 2.5 mm, the change of gradient can be seen. This phenomenon can be explained by the etching liquid climbing faster than dropping speed of specimen up to $x = 2.5$ mm, approximately due to a surface tension of the HF liquid. By the deconvolution process mentioned above, atomic concentration of all photoelectron peaks for the slope-shaped oxide film on SiC with respect to x-position were obtained, as shown in Fig. 5. The atom concentrations were derived by the first approximation using the ratio of the area intensity of the C-1s peaks to that of the pure C–Si peak, the same as C-1s for O-1s and Si-2p, using the ratio of O-1s peaks to O_2–Si peak and Si-2p peaks to Si^{4+} (or Si^{+}) peak. It is found that only when the thickness of oxide is ~2 nm, signals from the interface can be seen by XPS measurements. Taking account for the intensity ratio of Si^{0+} peak to Si^{+} peak, the thickness of the interface layer can be estimated to be one atomic layer or a few ones at most. From the results of Fig. 5, the depth where Si^{0+} photoelectrons come from is considered to be deeper from the surface than the depth where other interface photoelectrons come from, since Si^{0+} photoelectrons have the largest escape depth of all photoelectrons emitted from the interface. In addition, it is considered that Si–O–C bonds exist onto the Si–Si bonds since Si^{0+} peak disappears at thinner thickness of the oxide than the thickness which Si^{x+} disappears. If C–O bonds are a part of Si–O–C bonds, they also exist onto the Si–Si bonds.

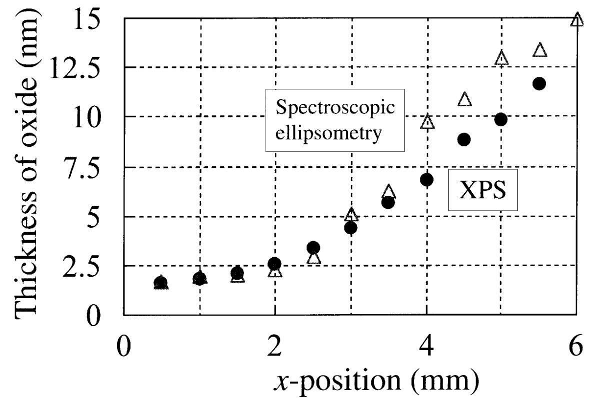

Fig. 4. Oxide thickness as a function of x-position measured by XPS (filled circle) and spectroscopic ellipsometry (triangle).

Table 1
All of the photoelectron peaks measured in this experiment

Composition spin	Bond	Binding energy (eV)	FWHM (eV)
Si-2p	Si–O_2	102.9–103.6[a]	1.10
	Si–O–C	101.50	0.80
	Si–C	100.6–101.2[a]	0.80
	Si–Si	99.00	0.85
C-1s	C–O	286.10	0.80
	$(CH_3)_n$	284.80	0.90
	C–Si	283.05	0.80
	C′	281.90	0.90
O-1s	O_2–Si, O–C	533.4–534.1[b]	1.10
	O′	531.00	1.35

[a] Denotes a lower shift with oxide decreasing.
[b] Denotes a higher shift with oxide decreasing.

Fig. 6 shows the values of E_b of all the photoelectron peaks with respect to x-position. It is found that Si^{4+} and Si^{0+} peaks shift to lower E_bs with decreasing the

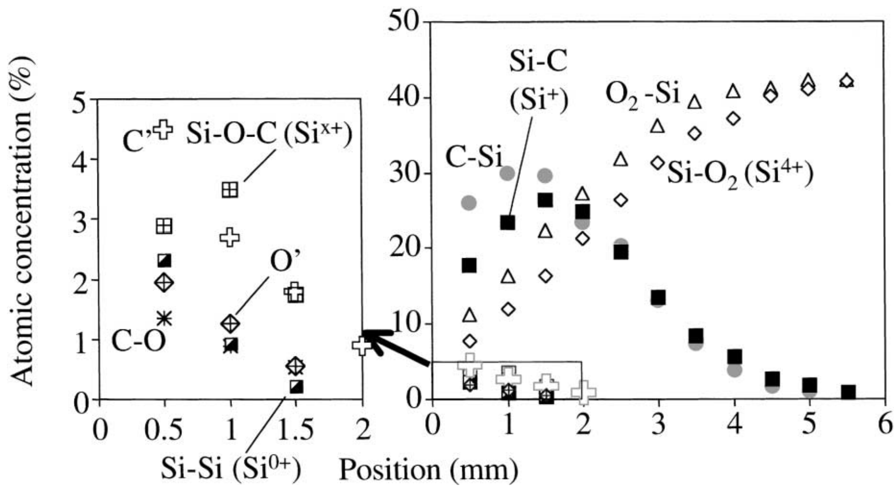

Fig. 5. The atom concentration for all elements as a function of x-position.

thickness of oxide. From this result, it can be considered that there exists a suboxide, which is often reported for the SiO_2/Si interface [18,19]. However, the suboxide is generally seen as a small shoulder peak between Si^{4+} and Si^{0+} (here, Si^{+}) peaks, and its intensity would be rather smaller than Si^{4+} or Si^{0+} peaks. Therefore, the presence of suboxide does not cause the change in E_b of Si^{4+} peak. Jernigan et al. [13] suggested that the shift of Si^{4+} peak is caused by the structural difference from a bulk SiO_2 due to the interfacial strain. Our results support their suggestion at present. However, our results in the motion of O_2–Si peak in O-1s spectra were different from their suggestion. They mentioned that the difference in E_b between Si^{4+} and O_2–Si is constant. However, the difference of E_b is not constant in our experiment. O_2–Si peak shifts to higher E_b with decreasing thickness of oxide, i.e., the peak shifts to the opposite direction from which Si^{4+} peak shifts. We have not discerned the origin of this difference, e.g., the difference of the oxidation

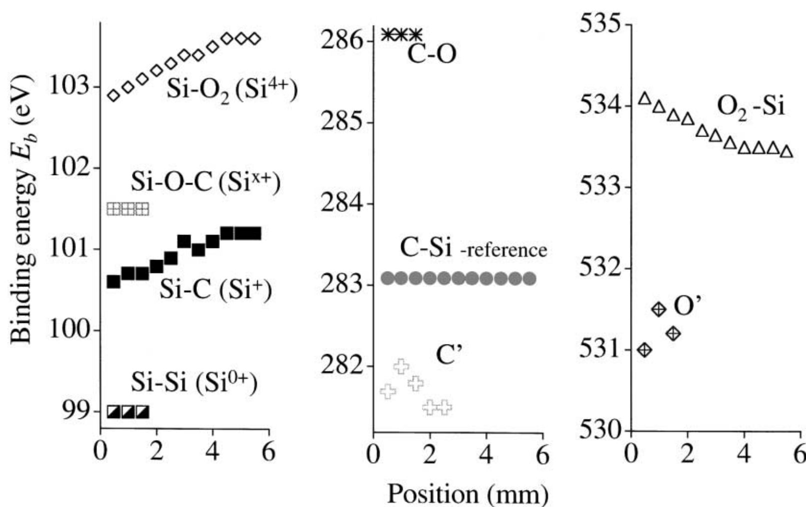

Fig. 6. Binding energy for all elements as a function of x-position.

process, that of the etching method, or that of the method of measurements. While, it has been reported that shift of Si^{+} peak can be explained by a Si–Si bond model [15]. Our observation of Si^{0+} near the interface is likely to support this model.

C–O and O′ bondings at the interface have a possibility to be gaseous CO and single oxygen atom, respectively. A post-oxidation anneal (POA) using high-temperature Ar ambient is able to remove the CO gas or O molecular from the interface. A reoxidation process (ROP) is considered to be effective to remove Si–Si bonds because the temperature of ROP is arranged at which SiC is difficult to be oxidized (<950 °C), and then only Si–Si bonds can be oxidized to SiO_2. An angle-resolved X-ray photoelectron spectroscopy (AR-XPS) may be useful to obtain the bond profile of oxide/SiC interfaces, since it is good for measuring in the depth scale of atomic layer level. Several additional experiments are required to reveal the interface layer completely.

4. Conclusions

XPS measurements have been done for shaped slope oxide film on 6H–SiC to characterize the oxide/SiC interface in terms of composition and bonds. We found that $Si–O_2$ and Si–C bond peaks shift to lower energy side with decreasing oxide thickness. Along with Si–Si bond, Si–O–C bond, C–O bond, new C-1s and O-1s peaks were detected at the oxide thickness less than 2 nm. Several interpretations for these results have been discussed. The structural difference due to the interfacial strain is considered as the origin of the shift of $Si–O_2$ peak, and the existence of Si–Si bond at the interface has a possibility to explain the shift of Si–C peak. C–O bonds are regarded as gaseous CO and/or a part of Si–O–C, and the extra O bonds at the interface have a possibility to be gaseous single oxygen atom.

Acknowledgements

This work was partly performed under the management of FED as a part of the METI Project (R&D of Ultra-Low-Loss Power Device Technologies) supported by NEDO.

References

[1] V.V. Afanas'ev, M. Bassler, G. Pensl, M.J. Sculz, Phys. Stat. Sol. A 162 (1997) 312.
[2] L.A. Lipkin, J.W. Palmour, J. Electron. Mater. 25 (1996) 909.
[3] K. Fukuda, S. Suzuki, T. Tanaka, K. Arai, Appl. Phys. Lett. 76 (2000) 1585.
[4] S. Sridevan, B.J. Baliga, IEEE Electr. Dev. Lett. 19 (1998) 228.
[5] D. Alok, P.K. McLarty, B.J. Baliga, Appl. Phys. Lett. 64 (1994) 2845.
[6] M. Yoshikawa, K. Saitoh, T. Oshima, H. Itoh, I. Nashiyama, Y. Takahashi, K. Ohnishi, H. Okumura, S. Yoshida, Mater. Sci. Forum 264–268 (1998) 1017.
[7] V.V. Afanas'ev, M. Bassler, G. Pensl, M.J. Sculz, J. Appl. Phys. 79 (1996) 3108.
[8] T. Iida, Y. Tomioka, Y. Hijikata, H. Yaguchi, M. Yoshikawa, Y. Ishida, H. Okumura, S. Yoshida, Jpn. J. Appl. Phys. 34 (2000) L1054.
[9] V.M. Bermudez, J. Appl. Phys. 39 (1989) 6084.
[10] B. Hormetz, H.-J. Michael, J. Halbritter, J. Vac. Sci. Technol. A 13 (3) (1995) 767.
[11] H. Tsuchida, I. Kamata, K. Izumi, Jpn. J. Appl. Phys. 34 (1995) 6003.
[12] C. Önneby, C.G. Pantano, J. Vac. Sci. Technol. A 15 (3) (1997) 1597.
[13] G.G. Jernigan, R.E. Stahlbush, M.K. Das, J.A. Cooper Jr., L.A. Lipkin, Appl. Phys. Lett. 74 (1999) 1448.
[14] M. Bassler, V.V. Afanas'ev, G. Pensl, Mater. Sci. Forum 264–268 (1998) 857.
[15] G.G. Jernigan, R.E. Stahlbush, N.S. Saks, Appl. Phys. Lett. 77 (2000) 1437.
[16] M. Yoshikawa, K. Saitoh, T. Oshima, H. Itoh, I. Nashiyama, S. Yoshida, H. Okumura, Y. Takahashi, K. Ohnishi, J. Appl. Phys. 80 (1996) 282.
[17] A. Namiki, et al., Surf. Sci. 203 (1988) 129.
[18] F.G. Bell, L. Ley, Phys. Rev. B 37 (1988) 8383.
[19] F.J. Himpsel, F.R. Mcfeely, A. Taleb-Ibrahimi, J.A. Yarmoff, Phys. Rev. B 38 (1988) 6084.